Updated Isoprene and Terpene Emission Factors for the Interactive BVOC Emission Scheme (iBVOC) in the United Kingdom Earth System Model (UKESM1.0)

James Weber[1], James A. King[1], Katerina Sindelarova[2], Maria Val Martin[1,3]

[1]School of Biosciences, University of Sheffield, Sheffield, S10 2TN, UK

[2]Department of Atmospheric Physics, Faculty of Mathematics and Physics, Charles University, Prague, Czech Republic

[3]Leverhulme Centre for Climate Change Mitigation, School of Biosciences, University of Sheffield, S10 2TN, Sheffield, UK

Correspondence to: James Weber (j.weber@sheffield.com)

Abstract.

Biogenic volatile organic compounds (BVOCs) influence atmospheric composition and climate and their emissions are affected by changes in land use and land cover (LULC). Current Earth System Models calculate BVOCs emissions using parameterisations involving surface temperature, photosynthetic activity, CO2 and vegetation type, and use emission factors (EFs) to represent the influence of vegetation on BVOCs emissions. We present new EFs for the *Interactive* BVOC Emission Scheme (iBVOC) used in the United Kingdom Earth System Model (UKESM), based on those used by the Model of Emissions of Gases and Aerosols from Nature (MEGAN) v2.1 scheme.

Our new EFs provide an alternative to the current EFs used in iBVOC, which are derived from older versions of MEGAN and the Organizing Carbon and Hydrology in Dynamic Ecosystem (ORCHIDEE) emission scheme. We show that current EFs used by iBVOC result in an overestimation of isoprene emissions from grasses, particularly C4 grasses, due to an oversimplification that incorporates the EF of shrubs (high isoprene emitters) into the EF for C3 and C4 grasses (low isoprene emitters). The current approach in iBVOCs assumes that C4 grasses are responsible for 40% of total simulated isoprene emissions in the present day, which is much higher than other estimates of ~0.3-10%.

Our new isoprene EFs substantially reduce the amount of isoprene emitted by C4 grasslands, in line with observational studies and other modelling approaches, while also improving the emissions from other known sources, such as tropical broadleaf trees. Similar results are found from the change to terpene EF.

With the new EFs, total global isoprene and terpene emissions are within the range suggested by literature. While the existing model biases in isoprene column are slightly exacerbated with the new EFs, other drivers of this bias are also noted. The

disaggregation of shrub and grass EFs provide a more faithful description of the contribution of different vegetation types to BVOC emissions, which is critical for understanding BVOC emissions in the pre-industrial and under different future LULC

35 scenarios, such as those involving wide scale reforestation or deforestation. Our work highlights the importance of using updated and accurate EFs to improve the representation of BVOC emissions in Earth System Models and provides a foundation for further improvements in this area.

1 Introduction

40 Biogenic volatile organic compounds (BVOCs) are emitted in large quantities by vegetation across the globe and undergo chemical reactions in the atmosphere. These reactions influence the atmosphere's radiative balance by perturbing atmospheric oxidant levels and thus the greenhouse gases methane and ozone as well as sulphate aerosol, and producing secondary organic aerosol (SOA). The influence of BVOCs on climate (Thornhill et al., 2021; Weber et al., 2022) necessitates accurate modelling of their emissions and the chemistry they undergo in global chemistry-climate models such as the United Kingdom Earth

45 System Model version 1 (UKESM1) used here.

Isoprene (2-methyl-1,3-butadiene) and monoterpenes (a range of molecules consisting of two isoprene units and referred to hereafter as terpenes for consistency with the nomenclature in the Interactive BVOC Emission Scheme - iBVOC) are the most widely emitted BVOCs yet there remains significant uncertainty in their total emissions. In the present day (PD), often taken

50 as the average over 1980-2014 or 2000-2014, global isoprene emissions estimates include 590 Tg yr^{-1} (Sindelarova et al., 2014), 440 Tg yr^{-1} (Sindelarova et al., 2022) with the majority of estimates falling in the range 450-620 Tg yr^{-1} (Fig 1, Messina et al., 2016). Averaged over 1980-2014, the mean of seven Earth System Models participating in the 6th Coupled Model Intercomparison Project (CMIP6) was 505 Tg yr^{-1} (range 67 Tg yr^{-1}) (Cao et al., 2021).

55 PD terpene emission estimates range from ~35 Tg yr^{-1} (Schurgers et al., 2009) to 160 Tg yr^{-1} (Guenther et al., 2012) with most estimates falling in the range of 90-135 Tg yr^{-1} (Messina et al., 2016).

Improvements to the understanding of the oxidation chemistry of isoprene (e.g., HO$_x$-recycling; Peeters et al., 2009; Wennberg et al., 2018) and terpenes (e.g., the formation of highly oxidised organic molecules (HOMs); Bianchi et al., 2019) over the last

60 decade have started to be included in global chemistry-climate models (e.g., CRI-Strat 2; Weber et al., 2021; MOZART TS2 Schwantes et al., 2020), helping to improve the simulation of BVOC chemistry in these models. Comparison of the atmospheric response to a doubling of BVOC emissions in UKESM1 when two different chemical mechanisms (one with basic BVOC chemistry, one with much more comprehensive BVOC chemistry including the recent advances to isoprene chemistry) were

used revealed how influential the modelling of chemistry can be on the simulated climatic impact of BVOCs (Weber et al., 2022). The warming effect of BVOC doubling was 43% smaller when using the more up to date BVOC chemistry in UKESM1.

While the simulation of BVOC chemistry is important for model performance, the emissions of BVOCs must also be simulated as faithfully as possible with inclusion of the dependencies on meteorology (temperature and solar radiation), atmospheric composition (CO_2) and land surface cover. Within climate models this simulation is often performed by specific modules such as iBVOC (Pacifico et al., 2011) or the Model of Emissions of Gases and Aerosols from Nature (MEGAN) v2.1 (Guenther et al., 2012) (more detail is provided in Section 2). These modules combine external variables (temperature, CO_2, photosynthetic activity etc.) with the vegetation distribution and vegetation-specific emission factors (EF) in a grid cell to calculate emissions of various BVOCs for that cell. The emission factors are the emission flux from a particular vegetation type per unit mass or area under a set of standard conditions and are typically derived from emission flux measurements from a range of specific vegetation species or an ecoregion as a whole (e.g., Guenther et al., 1995). Thus, emission factors provide a link between vegetation cover (i.e. LULC) and BVOC emissions and are central to simulating emissions accurately with incorrect values driving model biases. Updating emissions factors in UKESM is the major focus of this study.

The majority of isoprene and terpene emissions occur in the tropics with smaller contributions from temperate and boreal forests. Using MEGAN v2.1 with year 2000 simulated land cover from the Community Land Model version 4.0 (CLM4.0; Lawrence et al., 2011), Guenther et al. (2012) estimated that broadleaf evergreen tropical trees and broadleaf deciduous tropical trees account for 46% (51%) and 33% (28%) of total isoprene (monoterpene) emissions respectively.

C4 grass, which is also found in the tropics (e.g., in savannas) and mid latitudes, is believed to be a much weaker emitter of isoprene (e.g., Guenther et al., 2012; Loreto and Fineschi., 2015;) yet currently has an emission factor in iBVOC equal to that of tropical broadleaf evergreen trees, a known isoprene emitter. This is the major focus of the emission factor updates in this study and is discussed further in Section 2.

This study describes the development and evaluation of new emission factors for isoprene and monoterpenes for UKESM1. The work aims to improve the dependence of BVOC emissions on vegetation type and thus the description of biosphere – atmosphere interactions. While the primary focus of this work is isoprene emissions, for consistency we also propose updates to terpene emissions factors.

In Section 2 we first describe the current approach to modelling isoprene and terpene emissions in UKESM1 and highlight its limitations before detailing the calculation of new emission factors. In Section 3 we outline the model simulations performed to assess the impact of the new emissions factors and discuss the results in Section 4. Conclusions are presented in Section 5.

2 Development of New Emission Factors

2.1 iBVOC in UKESM1

UKESM1 is an Earth System model that couples individual component models which simulate the ocean, land surface, atmosphere and cryosphere (Sellar et al., 2020). Each component can also be run on their own (so-called "standalone"). The two components of relevance for this study are the land surface model (Joint United Kingdom Land Environment Simulator – JULES) (Best et al., 2011; Clark et al., 2011) and the atmospheric chemistry and aerosols model (United Kingdom Chemistry and Aerosols – UKCA; Archibald et al., 2020).

In JULES the land surface is described by dividing it into categories which can be grouped as vegetation (trees, grasses and shrubs) and non-vegetation (urban, bare soil, water, ice etc.) (Sellar et al., 2020). Depending on the configuration, there are between 5 and 13 types of vegetation, termed plant functional types (PFTs). Emissions of isoprene and terpenes are calculated using the Interactive BVOC Emission Scheme (iBVOC) (Pacifico et al., 2011), a module within JULES that reads in the simulated land surface. When running as part of fully-coupled UKESM1, emissions from iBVOC in JULES are passed to UKCA which simulates their addition to the atmosphere. When UKESM1 is run in atmosphere-only mode where vegetation cover is prescribed (along with sea-surface temperatures, sea-ice and ocean biogeochemistry), iBVOC can be used to calculate BVOC emissions from the prescribed vegetation and pass these emissions to UKCA. The latter configuration is used in this study.

Each PFT in UKESM1 has an associated emission factor (EF_{mass}) for isoprene (IEF_{mass}) and terpenes (TEF_{mass}) with units of mass of emitted carbon per leaf dry weight (dw) per hour ($\mu gC\ g_{dw}^{-1}\ hr^{-1}$). These EF_{mass} values represent the emission flux for a given PFT under the standard conditions specified in Pacifico et al. (2011) (30°C, 1000 $\mu mol\ m^{-2}s^{-1}$ of photosynthetically active radiation (PAR), 370 ppm CO_2). We note that subscript "mass" is used here to distinguish these emission factors from those with dimensions of mass per unit area of land surface per unit time (e.g., $\mu g\ m_{surface}^{-2}\ hr^{-1}$), which we are denoting as EF_{area} and are used in the MEGAN v2.1 scheme discussed later.

In iBVOC EF_{mass} are combined with other PFT-specific parameters, including photosynthetic activity and external variables including temperature and CO_2 concentration to calculate emissions of BVOC per PFT per grid cell. The dependencies on temperature, CO_2 concentration and photosynthetic activity are given in Pacifico et al. (2011).

iBVOC was first implemented with the original 5-PFT setup in UKESM1 which divides vegetated regions into the categories of Broadleaf trees, Needleleaf trees, C3 grass, C4 grass and Shrubs. IEF_{mass} values (Table 1) and the standard conditions were taken from Guenther et al. (1995).

When running JULES standalone over the period 1990-1999 these IEF_{mass} values yielded simulated total isoprene emissions of 535 TgC yr^{-1} (606 Tg yr^{-1}) with 9% coming from C4 grass (Pacifico et al., 2011).

135

To improve land surface modelling, configurations of JULES with 9 and 13 PFTs were developed with the 13-PFT approach the current standard in UKESM1 (Table 2) and the configuration used for UKESM1's contributions to the 6th Coupled Model Intercomparison Project (CMIP6) (Sellar et al., 2020). Going from the 5-PFT to the 13-PFT configuration, EF_{mass} values were assigned partly from those used in the 5-PFT configuration (e.g., the 13-PFT Broadleaf Deciduous Tree category has the same

140 IEF_{mass} as the 5-PFT Broadleaf Tree category) and partly from the Organizing Carbon and Hydrology in Dynamic Ecosystem (ORCHIDEE) vegetation scheme (Lathière et al., 2006). Unlike the 5-PFT configuration, the 13-PFT configuration does not appear to have been separately validated against observations or other model estimates and furthermore the IEF_{mass} of C4 grass was increased from 8 µgC g_{dw}^{-1} hr^{-1} to 24 µgC g_{dw}^{-1} hr^{-1} (Table 2).

145 In the context of this study, the limitation with using ORCHIDEE-derived EF_{mass} values for the 13-PFT configuration in UKESM1 is that the ORCHIDEE scheme does not simulate shrubs as a separate PFT. Rather the IEF from shrubs are incorporated into the IEF for C3 and C4 grass ORCHIDEE PFTs. This means the C3 and C4 grass PFTs in ORCHIDEE are not equivalent to those in UKESM1 and should not be used to provide the IEF values.

150 Lathière et al. (2006) noted that ORCHIDEE considers high IEF values for grasses and also acknowledged the high degree of uncertainty in this area, as several other studies have found low emissions of isoprene from grasses, and that a change to these values would lead to different regional distributions of emissions, a topic explored in Section 4.

In the updated version of ORCHIDEE, Messina et al. (2016) also notes the inclusion of shrubs in the EF values for the grass

155 PFTs in ORCHIDEE and it remains unclear whether the ORCHIDEE values for C3 and C4 grass are composed totally or only partially of the EF_{mass} from shrubs. Nevertheless, as UKESM1 simulates deciduous and evergreen shrubs as separate PFTs with their own emission factors, including the IEF_{mass} of shrubs into those for grasses is not correct.

Furthermore, as shrubs are relatively strong isoprene emitters (e.g., Lathière et al., 2006; Guenther et al., 2012), and C4 grasses

160 are not (e.g., Guenther et al., 2012; Loreto and Fineschi., 2015), this approach artificially increases the isoprene production potential from the UKESM1 C4 grass PFTs. This is exacerbated by the fact that large swathes of C4 grassland are in warm regions (e.g., sub-Saharan Africa and eastern Brazil), further increasing isoprene production given its strong temperature dependence (for example, isoprene emissions are 35% higher in iBVOC at 28°C than 25°C). Shrubs by contrast are typically found in higher latitude regions where the lower temperature leads to lower isoprene emissions, despite the relatively high

165 IEF.

2.2 MEGAN v2.1 in CESM2

The Community Earth System Model version 2 (CESM2) is another Earth System Model, which includes atmospheric, land, ocean and sea ice models that can be run in stand-alone or coupled configurations (Danabasoglu et al., 2020). The land model component is the Community Land Model version 5 (CLM5) (Lawrence et al. 2019), which also simulates BVOC emissions based on prevailing atmospheric conditions and land surface cover using MEGAN v2.1. The development of MEGAN is described in Guenther et al. (1995, 2006 and 2012). Like iBVOC, MEGAN v2.1 includes parameterisations for dependencies on temperature, CO_2 and PAR while also describing the impact of leaf age and soil moisture. A full description of the parameterisations is given in Guenther et al. (2012). CLM5 has 16 types of natural vegetation (including bare ground) and eight active crops. Similarly to JULES, vegetation and crops are represented by PFTs, each having specific ecophysiological, phenological and biogeochemical parameters (Lawrence et al., 2019). MEGAN v2.1 combines these parameterisations with PFT-specific emission factors (which for MEGAN are units in $\mu g\ m_{surface}^{-2}\ hr^{-1}$), to calculate BVOC emissions for a range of BVOCs. Furthermore, unlike ORCHIDEE, MEGAN v2.1 considers grasses and shrubs separately, with emission factors for each. This means the MEGAN EF for C3 and C4 grasses are more suitable as a starting point for calculating EF values suitable for iBVOC.

2.3 Calculation of EF$_{mass}$ from MEGAN for iBVOC

In this study, we use the MEGAN v2.1 EF (Table 3 Guenther et al., 2012) as it offers an alternative source of EF. We note that the same EF for isoprene are used in the more recently released version MEGAN v3.0 (e.g., Zhang et al., 2021). MEGAN v2.1 in CESM2 considers 15 PFTs (excluding bare soil) so we had to lump certain PFTs during the conversion to IEF for iBVOC to match the 13 PFTs classification in JULES. Table 3 shows the MEGAN v2.1 (CESM2) PFTs and the corresponding equivalents in iBVOC (UKESM1). Only 7 PFTs in MEGAN v2.1 have a direct equivalent in UKESM1, allowing direct calculation of the EF$_{mass}$; the other 8 PFTs were lumped into groups and the Crop 1 PFT in MEGAN v2.1 was used for the C3 and C4 crop and pasture PFTs in UKESM1.

EF in MEGAN are given in units of mass of species per unit area of land surface per unit time (e.g., $\mu g_{isoprene} m^{-2} hr^{-1}$), as opposed to $\mu gC\ g_{dw}^{-1}\ hr^{-1}$ used in UKESM1 and ORCHIDEE, and are denoted hereafter as IEF$_{area}$. Therefore, a conversion must be applied to make these values comparable to the EF used by iBVOC and ORCHIDEE, which are denoted as IEF$_{mass}$.

To convert EF$_{area}$ to EF$_{mass}$, we adapt Eq. 5 of Messina et al. (2016) to yield Eq. 1.

$$EF_{mass} = IEF_{area} \times \frac{1}{LAI_{ref}} \times \frac{1}{SLW} \times \frac{m_{Carbon}}{m_{species}} \times \frac{1}{C_{CE}}$$

$$(1)$$

Where LAI_{ref} is the reference leaf area index used by MEGAN v2.1 (5 $m^2_{leaf}\, m^{-2}_{surface}$), SLW is the specific leaf weight ($g_{dw}\, m^{-2}_{surface}$), the factor $\frac{m_{Carbon}}{m_{Species}}$ accounts for the fact that MEGAN v2.1 considers the mass flux of a given species and iBVOC and ORCHIDEE the mass flux of carbon and c_{CE} is the MEGAN canopy environment coefficient (0.57).

Eq. 1 is valid for emissions which are entirely dependent on PAR, as is the case for isoprene in MEGAN v2.1. Emissions of monoterpenes have a light-dependent fraction (LDF) and a light-independent fraction (IDF = 1 – LDF). In this case, Eq 1 needs to be modified to give Eq 2:

$$EF_{mass} = IEF_{area} \times \frac{1}{LAI_{ref}} \times \frac{1}{SLW} \times \frac{m_{Carbon}}{m_{species}} \times \left(\frac{LDF}{C_{CE}} + (1 - LDF) \right)$$

$$(2)$$

The LDF varies between species, and we used the values given in Table 4 of Guenther et al. (2012).

There are three main areas of uncertainty in the conversion: the lumping of PFTs, the choice of SLW values and, for terpene emissions, the choice of input TEF_{area} values.

2.3.1 PFT Lumping

We lump the MEGAN PFTs (Table 3) by calculating the mean EF value weighted by the area of each PFT. For example, the EF for the UKESM1 Needleleaf evergreen PFT is calculated as the mean of the MEGAN EF for Needleleaf evergreen temperate and Needleleaf evergreen boreal weighted by the total areas of these two species. We use the year 2000 LULC specified in Table 3 of Guenther (2012) for this lumping. The resulting EF_{area} value is then used in Eq. 1 to calculate EF_{mass}.

This approach necessarily introduces a dependency on the LULC assumption employed because different LULC datasets (i.e., CESM, ORCHDIEE, UKESM1 etc.) report different total areas for each PFT. We also acknowledge that LULC cover is likely to be different in past or future LULC scenarios, affecting the validity of the weighting to some degree. However, this impact

is expected to be small and would also occur if the ORCHIDEE scheme were used since it also has a greater speciation of
230   PFTs than UKESM1.

2.3.2 SLW values

One source of uncertainty in the EF_{mass}/EF_{area} conversion is the PFT-specific values of SLW. MEGAN v2.1 does not use SLW
(personal correspondence with Alex Guenther 6th April 2022), and we consider three other datasets of SLW from CLM5,
235   ORCHIDEE and UKESM1.

CLM5 uses specific leaf area (SLA in m^2 gC^{-1}) at the canopy top for photosynthesis calculations (Ali et al., 2016) and we
consider the inverse for SLW and apply a scaling of 2 to convert mass of carbon to dry leaf mass.
The ORCHIDEE BVOC scheme also reports SLA in units of m^2_{leaf} gC^{-1} (SLW in gC m^{-2}_{leaf}) (Table S1) . Similar to the CLM5
240   SLW, we apply a scaling of 2 to convert mass of carbon to dry leaf mass. For UKESM1, we use the reported values of SLW
(termed leaf mass area or lma) given in units of g_{dw} m^{-2} for the 13 PFTs.

Figure 1 shows the three SLW datasets with the CLM5 and ORCHIDEE values lumped into UKESM1 PFTs. We find
reasonable agreement, particularly between UKESM1 and CLM5 for the major emitting species.
245
To explore the uncertainty arising from the variation in SLW, we calculate EF_{mass} using the UKESM1, CLM5 and ORCHIDEE
SLW datasets. When calculating the EF_{mass} using the CLM5 and ORCHIDEE SLW values, we first calculate the EF_{mass} for the
scheme-specific PFTs (i.e., for the 15 PFTs in MEGAN) and then perform the lumping (Table 3). By contrast, when calculating
the EF_{mass} using the SLW which correspond to the UKESM's 13 PFTs, the EF_{area} from MEGAN v2.1 must be lumped first
250   before being converted to EF_{mass}.

2.3.3 Temperature Scaling

255   It is also necessary to consider the fact that the "standard conditions" differ between MEGAN v2.1, ORCHIDEE and iBVOC.

The temperature factor in MEGAN v2.1, γ_T, uses a parameterisation which considers the standard conditions for leaf
temperature ($T_s = 297$ K) and the average leaf temperature of the past 24 (T_{24}) and 240 (T_{240}) hours (Eq. 8-10; Guenther et al.,
2012). ORCHIDEE and UKESM1 assume that leaf and air temperature are the same and use standard conditions of 303.15 K
260   (30 °C). Therefore, it is necessary to scale the IEF_{mass} in Eqs. 1 and 2 to account for difference in standard temperature.

For isoprene emissions, iBVOC applies a temperature dependence (Eq. 3) (Pacifico et al., 2011) as:

$$T_{isop} = min[e^{0.1(T-303.15)}; 2.3]$$

$$(3)$$

In this work, we apply a temperature scaling, T_{isop_scale} (Eq. 4) using this temperature dependence to account for the difference in standard conditions.

$$T_{isop\_scale} = \frac{T_{isop@303.15K}}{T_{isop@297K}} = \frac{e^{0.1(303.15-303.15)}}{e^{0.1(297-303.15)}} = 1.85$$

$$(4)$$

iBVOC also applies a temperature dependence to terpene emissions (T_{terp}) in the 13-PFT setup for all PFTs, except for Broadleaf Deciduous trees whose parameterisation we describe later (Pacifico et al., 2011) (Eq. 5).

$$T_{terp} = e^{0.09(T-303.15)}$$

$$(5)$$

Following the same approach as for isoprene emissions, we apply a scaling factor T_{terp_scale} (Eq. 6).

$$T_{terp\_scale} = \frac{T_{terp@303.15K}}{T_{terp@297K}} = \frac{e^{0.09(303.15-303.15)}}{e^{0.09(297-303.15)}} = 1.74$$

$$(6)$$

In iBVOC terpene emissions for Broadleaf Deciduous trees are assumed to have a PAR-independent component and a PAR-dependent component (terpene emissions for all other PFTs are assumed to be entirely PAR-independent). In a similar approach to MEGAN v2.1 (Section 2.2; Guenther et al., 2012), the PAR-independent component uses the terpene temperature dependence (T_{terp}; Eq 5) while the PAR-dependent component uses the isoprene temperature dependence (T_{isop}; Eq. 3) along with an additional term representing photosynthesis. These components have a 50:50 weighting and we therefore use an average of T_{isop_scale} and T_{terp_scale} for the temperature scaling, $T_{terp\ BrDe\_scale}$, for this PFT (Eq. 7).

$$T_{terp\_BrDe\_scale} = 0.5T_{terp\_scale} + 0.5T_{isop\_scale} = 1.79$$

$$(7)$$

It is important to note that MEGAN v2.1 uses a more complicated temperature dependence which considers average leaf temperatures over the previous 24 and 240 hours. MEGAN v2.1 and iBVOC also differ in their simulation of CO_2 inhibition (which is PFT-specific for iBVOC but not in MEGAN) and photosynthesis. Both models simulate reductions in isoprene emissions with CO_2. The CO_2 inhibition parameterisation in iBVOC follows that of Arneth et al (2007), considering the ratio of the plant's internal CO_2 concentration to a PFT-specific reference value, while MEGAN uses the parameterisation of Heald et al (2009) which is not PFT-specific. Cao et al (2021) found the CO_2 inhibition in UKESM (using iBVOC) to be almost twice that of CESM (using MEGAN) when considering isoprene emissions in the late 21st century. MEGAN parameterises the effect of photosynthesis with a scaling term composed of a light dependent fraction (LDF) and light independent-fraction (LIDF = 1-LDF) with the former a function of the photosynthetic photon flux density averaged over a 24-hour period for both shaded and unshaded leaves (Section 2.2, Guenther et al., 2012). By contrast, iBVOC describes the impact of photosynthesis from the perspective of electron transport, following Arneth et al (2007) as described in Section 2.2 of Pacifico et al (2011). MEGAN v2.1 also features a parameterisation to account for the influence of leaf age on emissions while iBVOC does not. Accounting for these parameterisation differences is very complicated and has not been done in this conversion.

2.3.4 EF for terpene emissions

For terpenes a further factor in the conversion must be considered. Unlike isoprene where the tracer in UKCA corresponds directly to the molecule isoprene, the one or two terpene tracers in UKCA actually represent a wide range of monoterpene species.

The Strat-Trop (ST) chemistry scheme (Archibald et al., 2020), the standard in UKESM1, considers a single tracer, Monoterp (MT), whose initial oxidation reactions with OH, O_3 and NO_3 have the rate constants of the most widely emitted monoterpene, α-pinene. The alternative mechanism, CRI-Strat 2 (CS2) (Weber et al., 2021) considers separate α-pinene and β-pinene tracers which have different rate constants. When using the ST mechanism, terpene emissions calculated by iBVOC are mapped directly to MT emissions considered by UKCA while in CS2 terpene emissions are split in a 2:1 ratio for α-pinene and β-pinene, representing the approximate global emissions ratio of these species (Sindelarova et al., 2014).

MEGAN v2.1 provides separate PFT-specific EF$_{area}$ for α-pinene, β-pinene, myrcene, sabinene, limonene, 3-carene and t-β-ocimene and for an "other monoterpenes" category. For the major emitting PFTs the EF$_{area}$ of α-pinene are ~60% higher than those of β-pinene and 2-3x higher than those of the other specific monoterpenes (e.g., myrcene) and the "other monoterpenes" category. Since the emissions of MT in ST and α-pinene and β-pinene in CS2 represent all monoterpenes, a choice must be made regarding how to combine these EF$_{area}$.

In this analysis, we consider three options – using only the α-pinene EF_{area}, using the α-pinene and β-pinene EF_{area} in a 2:1 weighted mean (representing the ratio of these species in Sindelarova et al., 2014) or using the α-pinene, β-pinene and "other

330 monoterpenes" EF_{area} in a mean weighted by the total emission estimates in Sindelarova et al. (2014), namely 32 : 16.7 : 46.3. Sindelarova et al. (2014) does not speciate monoterpenes beyond α-pinene, β-pinene and total monoterpenes so inclusion of the EF_{area} of the other species like myrcene was not considered here.

335 **2.3.5 EF_{mass} values**

Figure 2 shows the PFT-specific EF_{mass} values for isoprene (IEF_{mass}) and terpene (TEF_{mass}) calculated using the SLW datasets and, in the case of TEF_{mass}, the three different combinations of monoterpene EF from MEGAN v2.1. We also show the current IEF_{mass} and TEF_{mass} used by UKESM1.

340

Unsurprisingly, the new approach yields substantially lower EF_{mass} values for C4 grass, crops and pasture compared to the UKESM1 default. The IEF_{mass} of needleleaf deciduous trees decreases to almost zero (its IEF_{area} has the joint lowest value in MEGAN v2.1) while the IEF_{mass} and TEF_{mass} of all broadleaf trees increase.

345 The variation in EF_{mass} from uncertainty in SLW is particularly notable for the broadleaf deciduous and broadleaf evergreen temperate PFTs but smaller for the broadleaf evergreen tropical PFT, the single largest emitter of isoprene. The impact of this uncertainty on isoprene emissions is explored by comparing emissions from UKESM1 simulations using the IEF_{mass} calculated using UKESM1 SLW and CLM5 SLW (Table 4; Evaluation). This was not done for terpene emissions since the choice of EF_{area} is likely to be a much larger source of uncertainty.

350

3 Evaluation Simulations

To assess the impact of changing the EF_{mass} values we performed a range of simulations in UKESM1 with varying IEF_{mass} and

355 TEF_{mass} values and two accompanying simulations in CESM2 for comparison purposes We also evaluated the resulting simulated isoprene columns against satellite observations from the Cross-track Infrared Sounder (CrIS) and ground observations. Tables 4 and 5 summarise the simulations performed for this evaluation.

360 **3.1 UKESM1 Simulations**

All UKESM1 simulations used the atmosphere-only configuration of UKESM1 run at a horizontal resolution of 1.25°×1.875° with 85 vertical levels up to 85 km (Walters et al., 2019), and the GLOMAP-mode aerosol scheme, which simulates sulfate, sea salt, BC and organic matter, but does not simulate currently nitrate aerosol (Mulcahy et al., 2020).

365 Mineral dust is simulated using the bin scheme of Woodward (2001). UKESM1 has the capability to perform simulations using specified dynamics, also called "nudging", where certain offline meteorological fields from the ERA-Interim reanalysis(temperature and horizontal winds) are input (Dee et al., 2011), and free-running with online computed meteorology..

Our evaluation has three sections. Firstly, we perform present day (PD) simulations nudged to atmospheric reanalyses to
370 compare the model simulations with different EF_{mass} values to observational data (Table 4). Secondly, we perform free-running simulations using conditions from the pre-industrial (PI) and Shared Socioeconomic Pathway SSP3-7.0, which represents a "regional rivalry" scenario, at 2050 (O'Neill et al., 2016) to assess the effect these different EF_{mass} values would have at these two periods (Table 4). Finally, we perform free-running simulations using PD conditions but with LULC from either the PD or specific future LULC scenario featuring widescale re/afforestation to assess the impact these EF_{mass} values would have on
375 the response of mass tree planting (Table 5). Runs used the CS2 chemical mechanism (Jenkin et al., 2019; Weber et al., 2021), version 12.0 of the Unified Model (UM) and vn6.1 of JULES.

Nine 1-year PD simulations were performed for November 2012 – October 2013 as this period covers 4 months for which there exists satellite CrIS observations of global isoprene column (January, April, July and October 2013; Wells et al., 2020).
380 Six runs were performed to evaluate plausible EF_{mass} approaches by comparison of the resulting total global emissions to estimates from other sources and, for isoprene, comparison of simulated column values against measured column values. No_C4_emiss_PD was run to isolate the fraction of emissions from C4 PFTs (see Section 4). Finally, two 3-year nudged PD simulations were run with UKESM1 default EF_{mass} and the proposed new EF_{mass} to ensure the trends established in the 1-year runs were not simply caused by the prevailing meteorology and persisted over a longer period. We also performed two
385 UKESM1 simulations using LULC taken from a PD CESM2 simulation (with PFTs lumped as described in Section 2) to assess the influence of the underlying simulated LULC on emissions. These simulations, IEF_SLW_UKESM_PD_CESM_LULC and IEF_SLW_CLM5_PD_CESM_LULC (Table 4), used the same IEF values as IEF_SLW_UKESM_PD and IEF_SLW_CLM5_PD respectively.

390 Nudging of temperature and horizontal wind was used to prevent diverging meteorology affecting BVOC emissions as well as replicating as closely as possible the atmospheric conditions experienced when the observations were recorded. Thus nudging, along with the use of observed sea surface temperature (SSTs) fields, means that, as far as possible, the changes in EF_{mass} will be the only drivers of emission changes and allows for a more faithful comparison to observational data. Nudging only occurred above ~1200 m in altitude, and thus most of the planetary boundary layer was not nudged.

395

The 1-year PD nudged runs used timeseries of anthropogenic and biomass burning emissions to keep the simulated conditions as close to those when the observations were recorded. The 3-year nudged PD runs used 2014 timeslice anthropogenic and biomass burning emissions. All these simulations used prescribed LULC from a UKESM1 historical ensemble member performed for CMIP6 (Sellar et al., 2020).

400

The four free running simulations performed to investigate how the EF_{mass} changes would affect simulated emissions in the PI and in 2050 under conditions used prescribed LULC from the UKESM1 piControl and SSP3-7.0 runs performed for CMIP6 (Sellar et al., 2019) and timeslice emissions from 1850 and SSP3-7.0 2050 respectively (Table 4).

405 We also explored how the change to EF_{mass} would affect the response to a specific LULC change with a further set of simulations, which used two time periods from a specific land use scenario featuring widescale afforestation and reforestation ("MaxForest"). The Maxforest scenario features a very high degree of reforestation and afforestation over the course of the 21st Century and was developed to assess the impact of such LULC with regards to carbon sequestration, among other factors. The scenario gradually expands existing forested regions with suitable tree species and also avoids encroachment on cropland, 410 pastures and urban regions. It can thus be considered as a scenario representing a near maximum plausible level of re/afforestation. The Maxforest scenario was originally developed for CLM5 (Lawrence et al. 2019) and we adapted it for UKESM1 using the same lumping of PFTs as discussed in Section 2.3.1. We performed simulations with the default and new EF_{mass} values with LULC from the start of the MaxForest scenario at 2010 (no increase in tree cover) and at 2050 when extensive reforestation was well underway. All these simulations used PD anthropogenic and biomass burning emissions and 415 GHG concentrations but BVOC emissions were allowed to respond to LULC change. We compare the change in isoprene and terpene emissions between 2010 and 2050 Maxforest land use when the default EF_{mass} values were used to when the new EF_{mass} values were used. We also performed the same experiments in CESM2 (Section 3.2) and compare the change in BVOC emissions between 2010 and 2050 Maxforest land use to the UKESM simulations.

420 In all runs CO_2 was not emitted but set to a constant field appropriate for the PI, PD and 2050 under SSP3-7.0 conditions, while the other well-mixed greenhouse gases (WMGHGs) CH_4, CFCs, and N_2O were prescribed with constant lower boundary conditions (Archibald et al., 2020) appropriate for the PI, PD and 2050 under SSP3-7.0 conditions.

Fields for sea surface temperatures (SSTs), sea ice (SI), ocean biogeochemistry (DMS and chlorophyll) were prescribed for 425 all runs. The nudged PD runs used observed SSTs and SI and ocean biochemistry from a UKESM1 historical ensemble member. The free-running PI runs used a 30-year mean from the UKESM1 piControl for SSTs, SI and ocean biogeochemistry. The SSP3-7.0 2050 runs used 2050 ocean biogeochemistry and 2045-2055 mean SSTs and SI, all taken from one of the UKESM1 SSP3-7.0 ensemble members.

430   The free running Maxforest simulations (Table 5) used 2050 ocean biogeochemistry, 2045-2055 mean SSTs and SI and PD anthropogenic emissions and prescribed concentrations of WMGHGs. The same SSTs and WMGHG concentrations were applied to ensure differences in BVOC emissions were due to LULC only.

435   All UKESM1 runs used oceanic emissions of CO, C_2H_4, C_2H_6, C_3H_6 and C_3H_8 from the POET 1990 data set (Olivier et al., 2003), and all biogenic emissions except isoprene and monoterpenes were based on 2001–2010 climatologies from the MEGAN-MACC dataset (Sindelarova et al., 2014) calculated by the MEGANv2.1 model (Guenther et al., 2012) under the Monitoring Atmospheric Composition and Climate project (MACC). Emissions of isoprene and monoterpenes (split in a 2:1 ratio between α-pinene and β-pinene) were calculated interactively using iBVOC. Anthropogenic and biomass burning emissions data for CMIP6 are from the Community Emissions Data System (CEDS), as described by Hoesly et al. (2018).

440

3.2 CESM Simulations

     The CESM simulations used version 2.2.0 (Danabasoglu et al. 2020) at a 0.9° x 1.25° horizontal resolution. For the atmospheric component, we employ CAM-chem version 6 (hereinafter CAM6-chem), with a full tropospheric O_3–NO_x–CO–VOC–aerosol
445   chemistry based on an updated tropospheric chemistry mechanism (MOZART-TS1) (Emmons et al 2020) with the Modal Aerosol Model with 4 modes (MAM4) (Liu et al., 2016). CAM6-chem has 32 vertical layers and a model top of ~45 km, and is coupled to CLM5, which provides BVOCs with the MEGAN v2.1 scheme and handles dry deposition. Our simulations used specified sea surface temperatures and thermodynamic sea ice.

450   For the two CESM simulations, anthropogenic and biomass burning emissions of reactive gases and aerosols were fixed to a 2010 climatology (2006-2014 average) using data from Hoesly et al. (2018). WMGHGs were incorporated as fixed lateral boundary conditions rather than as emissions from the surface and were also fixed to 2010 values (2006-2014 average) using standard concentration data from CMIP6 (Meinshausen et al. 2017).

455   For LULC, we performed the same free-running PD and 2050 LULC simulations as in UKESM1 (Table 5) to allow comparison of the BVOC emission responses to the LULC change in UKESM1 and CESM. As with UKESM1, the CESM simulations were atmosphere-only and used PD anthropogenic emissions and prescribed WMGHG concentrations and 2045-2055 mean SSTs with the only difference between the simulations being the LULC.

460   **3.3 Observational Data**

Monthly mean isoprene columns derived using the space-borne CrIS technique (Wells et al., 2020) were used as the principal method of evaluation since it all allows the regional changes to be readily assessed. The CrIS is a longwave infra-red Fourier

transform spectrometer onboard a satellite which can measure two isoprene IR absorption features. The absorption data collected by the spectrometer are then combined with an artificial neural-network to calculate isoprene columns.

465

Surface isoprene emission measurements from regions with C4 grass were also used to examine the impact of substantial reduction in C4 grass IEF_{mass}. In lieu of observations from C4-only regions (which are very sparse given the understanding that C4 grasses are weak isoprene emitters), we use observations from savanna, which tends to comprise grasses, woody shrubs and a range of trees, including strong isoprene and monoterpene emitters (e.g., Table 3 Otter et al., 2002), in varying
470   proportions. We select savanna observations from sites specifically noted to be without dominant isoprene emitters (Central Africa Republic - Klinger et al., 1998; Nylsvley, South Africa Guenther et al., 1996 and Otter et al., 2002). We note that these sites were likely to have grass species with very low isoprene emissions, below the instrument detection limits (e.g., Harley et al., 2003). Therefore, our compiled observations represent an upper bound for isoprene emissions from C4 grass.

475   We also used monoterpene emission data measured at the SMEAR II site in Hyytiälä (https://smear.avaa.csc.fi; last accessed 19th March 2023) to evaluate the change in terpene emissions.

4 Results

480   The impact of changing EF_{mass} values is assessed in terms of total isoprene and monoterpene emissions and, in the case of isoprene, against global isoprene column values. We also discuss change in the contribution to total emissions from the different PFTs and the impact of the EF_{mass} changes on simulated emissions in the PI, at 2050 under SSP3-7.0, and the re/afforestation LULC scenario.

485   **4.1 Total Global Emissions**

Table 4 presents the global isoprene and terpenes emissions in our simulations. For isoprene, all nudged PD simulations, except No_C4_emiss_PD, yield total emissions within the range of previous estimates. Simulations using IEF_{mass} from UKESM1 SLW ("IEF_SLW_UKESM_PD") and CLM5 SLW ("IEF_SLW_CLM5_PD") yield emissions 13% and 7% lower than the
490   UKESM1 control simulation ("Control_1yr_PD"), respectively.

When UKESM1 LULC was replaced with CESM2 LULC, isoprene emissions are 380 Tg yr^{-1} (IEF_SLW_UKESM_PD_CESM_LULC) and 420 Tg yr^{-1} (IEF_SLW_CLM5_PD EF). These values are lower than the 457 Tg yr^{-1} and 490 Tg yr^{-1} simulated using the same IEF values and UKESM LULC, yet they are still well within the range of
495   simulated emissions (310-680 Tg yr^{-1}) of Fig 1 of Messina et al (2016). This highlights the influence of uncertainty in LULC on BVOC emissions but, as iBVOC is chiefly for use with UKESM1, we will focus on the simulations using UKESM1 LULC.

For terpenes, when the TEF_{mass} is based solely on α-pinene (TEF_AP_PD), total emissions (177 Tg yr^{-1}) are higher than
previously published results (Messina et al., 2016) and when the TEF_{mass} is derived from the weighted average of ratio of α-pinene, β-pinene and other monoterpenes" (TEF_all_PD), total emissions (88 Tg yr^{-1}) are at the lower end of estimates. However, when taking a 2:1 ratio of α-pinene and β-pinene TEF_{area} (TEF_AP_BP_PD), the resulting emissions (130 Tg yr^{-1}) are more in line with other estimates.

The clearest indication of the significant contribution C4 PFTs make to BVOC emissions in the current UKESM1 setup comes from the comparison of the Control_1yr_PD and the No_C4_emiss_PD, where the EF_{mass} of all C4 PFTs is zero, simulations. This reveals that C4 PFTs contribute about 40% (18%) to total isoprene (terpene) emissions in the current UKESM1 setup, far higher than the 1% (0.3%) estimated by Guenther et al. (2012), 9% for isoprene from the original 5-PFT version of iBVOC (Pacifico et al., 2011) and 1-2% for isoprene estimated by Pfister et al. (2008). As previously discussed, this substantial contribution from C4 grasses is also in stark contrast to other studies, which highlight very low emissions of isoprene from C4 grasses (e.g., Loreto and Fineschi., 2015). Overall, this suggests that while the current UKESM1 approach may produce a reasonable value for total isoprene and terpene emissions, these are derived using unrealistic EF for C4 grasses.

With the updated EF_{mass}, C4 grass PFT contributes 1-3% of total isoprene emissions (based on chosen SLW) and 0.2-0.7% of total terpene emissions (based on choice of EF_{area}), bringing UKESM1 into line with other estimates.

The decreases in C4 PFT EF_{mass} and increases in the EF_{mass} of the broadleaf evergreen tropical tree PFT leads to the contribution to total isoprene emissions from broadleaf evergreen tropical trees increasing from 45% to 75% (50% to 80% for terpenes). This contribution is greater than the 46% estimated by MEGAN v2.1 (Guenther et al., 2012). However, the area of this PFT in UKESM1 is 67% greater than CLM4 (26.0 vs. 15.6×10^6 km^2). (While this difference in area may seem large, the total areas of tropical trees in UKESM and CLM4 are much more similar if the area of CLM4's deciduous evergreen tropical tree PFT, for which is there is no direct analogue in UKESM, is included.) On an emissions per unit area basis for the broadleaf evergreen tropical PFT, isoprene emissions in UKESM1 are within 5% of that from Guenther et al. (2012) while terpene emissions are ~25% lower. This separately highlights the important issue of uncertainty in land use and land cover and the effect that it can have on model-model comparisons (e.g., in CMIP6) and model-observation comparisons.

Spatially, the new IEF_{mass} led to isoprene emission increases across Amazonia (albeit with a small reduction around Manaus) and Congo, and decreases north and south of the African rainforest where the simulated C4 grass PFT dominates (Fig 3(a)). Terpene emissions increase over the tropics due to increases in the TEF_{mass} of tropical evergreen broadleaf trees, while they

530 decrease in mid- and high-latitudes (Fig 3(b)) from reductions in the TEF_{mass} of needleleaf evergreen and deciduous PFTs (Fig 2(b)).

For the PI and future simulations with UKESM1 (Fig S1), the new EF_{mass} values lead to reductions in total global isoprene (terpene) emissions of 13% (11%) and 8% (8%) in the PI and 2050 SSP3-7.0 scenarios respectively compared to the default

535 EF_{mass} (Base PI). For both scenarios, isoprene emissions from C4 PFTs decrease by ~90%, while emissions from broadleaf evergreen tropical trees increase by ~50%. This leads to emission increases over Amazonia and Congo, but decreases north and south of the Congo (Fig S1(a,c)). Terpene emissions from C4 PFTs drop to almost zero and decrease by ~60% from needleleaf evergreen trees, while increasing by around 50% from broadleaf evergreen tropical trees, driving a tropical emission increase and high latitude emission decrease (Fig S1(b,d)).

540

4.2 Isoprene Column Comparison

We compare the output from the PD simulations to the CrIS observed isoprene columns (Section 3.3) for January, April, July

545 and October 2013 (Fig 4). The use of nudging significantly reduces the difference in meteorology between the simulations and reality, greatly improving the comparability of modelled and observational data. However, the lowest 11 model levels (approx. 700-1000 m) are not nudged so there will be some differences between the model simulation conditions and reality in the boundary layer, although this is tempered by the nudging applied to the higher levels.

For the 4 months considered, IEF_SLW_UKESM_PD and IEF_SLW_CLM5_PD yield lower total isoprene emissions than

550 the Control_1yr_PD, but show generally slightly higher columns biases in the same regions where the control run has a bias, chiefly in Western Amazonia.

This bias exacerbation is slightly greater in IEF_SLW_CLM5_PD than IEF_SLW_UKESM_PD and is likely driven by the increase in IEF_{mass} for the tropical broadleaf evergreen trees which are dominant in the region. The biases over central Africa

555 are very similar between the three approaches.

The increased biases with the new IEF_{mass} (e.g., the increase of 0.5-0.7×10^{15} molecules cm^{-2} over South America in January 2013. Fig 4(a-c)) is not necessarily indicative of these new IEF_{mass} values being less accurate than the original IEF_{mass} values which may be performing better due to offsetting issues. Biases in LULC, as highlighted by the comparison of UKESM1 and

560 CLM5 in terms of broadleaf versus deciduous tropical trees, simulated chemistry and emissions of other species (e.g., NO_x) which affect the atmospheric oxidising capacity and thus isoprene concentrations will also contribute to the enhanced model bias. The difference in model bias between simulations with the default and new IEF_{mass} values is noticeably smaller than the difference in the model bias when different chemical mechanisms are used. For example, in April 2013, the mean bias over

South America in the Strat-Trop mechanism (Archibald et al., 2020) was 5.7×10^{15} molecules cm^{-2} and this decreased substantially to 0.6×10^{15} molecules cm^{-2} when CS2 was used (Figure 2; Weber et al., 2021)

4.3 C4 Emission Observation Comparison

Given the major change to the IEF$_{mass}$ values of C4 grass, the isoprene emissions from C4 grasses were compared to observations in southern Africa (Section 3.3, Fig 5). The model resolution (~100 x 100 km in the region of relevance) means the grid cells where observations were taken contained high fractions of strong isoprene emitters, typically broadleaf evergreen tropical trees, as well as C4 grasses. To isolate the impact of C4 grass emissions we take the area-weighted mean of emissions from grid cells in the region where C4 grasses comprise > 80% of the total surface types (vegetation and non-vegetation). We use the 3-year monthly mean for the month when observations were recorded and apply a scaling factor of 2 to account for the fact that isoprene emissions are zero at night. (Emission measurements were only taken during the day while the use of model monthly average values mean that approximately half of the data points going into the model value will been zero, halving the model's average.)

While comparison of these model and observational data should be treated as illustrative rather than definitive for the reasons explained above, it suggests that the reduction in C4 IEF$_{mass}$ may help to reduce the model high bias in C4 grass dominant regions. We also note that the observed values represent an upper bound since the emissions in some regions will be below the limit of detection (e.g., Harley et al., 2003).

4.4 Terpene Emission Evaluation

While the primary focus of this paper is correcting the error with the emission factors for C4 grasses, we also performed a comparison of monoterpenes emissions measured by the SMEAR II station in Hyytiälä in the boreal forest, with emissions from simulations using the current TEF$_{mass}$ (Control_1yr_PD) and updated TEF$_{mass}$ (TEF_AP_BP_PD) values. We found that new the TEF$_{mass}$ yielded emissions which compared well to observations (Fig S2).

4.5 Impact on response to LULC Changes

Tropical broadleaf evergreen trees and C4 grass PFTs are some of the most widespread vegetation types in the tropics. The respective increase and decrease in EF$_{mass}$ values for these PFTs means the response of BVOC emissions to a change in the relative fractions of these species is likely to be quite different when using default and new EF$_{mass}$ values. We explored this further using UKESM1 and CESM and the MaxForest scenarios since this scenario involves, among other changes, increases to tropical broadleaf evergreen tree cover at the expense of C4 grasses in Africa and eastern Brazil (Fig S3 and Table 5).

When the UKESM1 default EF_{mass} values are used, the extensive re/afforestation in the Maxforest scenario yields a reduction in isoprene emissions relative to 2010 (Fig 6(a)). This is due to the decrease in C4 grass coverage shown by emission reductions in regions where C4 grasses are replaced by trees. By contrast, when the updated EF_{mass} values are used, the Maxforest scenario leads to an increase in isoprene emissions in UKESM1 (Fig 6(b)) which resembles the response simulated in CESM (Fig 6(c)). The similarity between the responses in UKESM1 with the new EF_{mass} and CESM is not surprising since CESM also uses the MEGAN v2.1 scheme for the emissions of isoprene.

4.6 Recommended EF_{mass}

For isoprene, there is little to differentiate the approaches using SLW from CLM5 or UKESM1. The CLM5 SLW approach yields slightly higher column biases but total PD emissions (491 vs 457 Tg yr^{-1}; Table 4) which are closer to median of other estimates (~500 Tg yr^{-1}; Messina et al., 2016). The CLM5 SLW approach allows PFT-specific SLW values to be used to calculate the EF_{mass} of the MEGAN v2.1 PFTs before they are lumped into UKESM PFTs while using the UKESM1 SLW values means lumping must occur before the EF_{mass} are calculated, potentially increasing uncertainty in the output. Overall, we tentatively recommend using the IEF_{mass} values calculated using the CLM5 values (i.e. IEF_SLW_CLM5_PD). For terpenes, based on total emissions we recommend the TEF_{mass} calculated from the TEF_{area} of α-pinene and β-pinene in 2:1 ratio (Guenther et al., 2012), i.e., those used in TEF_all_PD. These EF_{mass} values are given in Table 6.

We do not claim that the new EF_{mass} values are the final word on the matter; rather we believe they represent an improvement over those currently used in UKESM1 and provide a clear method for recalculation in the future should revised EF_{area} values be developed and/or a wider range of PFTs considered.

4.7 Uncertainties and Future Work

Accurate modelling of BVOC emissions depends on the parameterisations within the emission module (in this case, iBVOC) and the simulations of external factors, which influence emissions. This study deals with just one part of this framework: biases in these external factors can limit the effectiveness of model-observational comparisons, such as the satellite-derived isoprene columns shown in Figure 4, and offsetting errors can lead to reasonable results, at a given period in time, or improvements to certain components (e.g., emission factors) yielding reductions in model performance. Nevertheless, progress towards an approach that faithfully captures biosphere-atmosphere interactions requires incremental improvements to all contributing factors. Here we describe some other sources of uncertainty in the simulation of BVOCs and areas where future work would be useful.

iBVOC includes dependencies on CO_2, temperature, photosynthetic activity and plant functional type, with the latter the focus of this study. MEGANv2.1 considers the role of leaf age on emissions and leaf temperature over the past 24 hours and 240 hours while these factors are omitted in iBVOC: assessing the impact of these parameterisations in iBVOC would be worthwhile.

Within the parameterisation of PFT dependency updated in the study, several areas of uncertainty have been identified. The impact of SLW value variations and the multiple options regarding which TEF$_{area}$ values to use has been quantified with the range of simulations performed in this work. Other areas of uncertainty have not been fully scrutinised due to a relative lack of observational data. Compared to the species which are strong isoprene emitters, observations of emissions from grasses are sparse, hindering further model validation. MEGAN v2.1 also prescribes a single, very small EF$_{area}$ for all crops and pasture, resulting in negligible emissions from these PFTs. Emissions from longer-lived crops and pasture are likely to tend towards grasses and the projected expansion of these PFTs in some future scenarios, particularly those with increasing population, means capturing emissions from these PFTs may become more important. Further observations would aid in this effort. We also note that the emission factors in MEGAN v2.1 are not perfect and will continue to be refined. For example, Sindelarova et al (2022) updated emissions factors for α-pinene for certain tree PFTs. For consistency, the MEGAN emissions factors used in this study are all from MEGAN v2.1 but future development of iBVOC should take into account the latest understanding of emission factors.

Simulation of external factors including land cover (cf. the effect of swapping UKESM and CESM LULC on simulated emissions; Table 4), surface temperature and meteorological conditions (e.g., droughts and floods) also affect BVOC emissions (eg, Sheil., 2018; Yáñez-Serrano et al., 2020).

The reduced nature of Earth System models requires the aggregation of a wide range of vegetation types, which in reality have varying emission factors, into a small number of PFTs. This oversimplification can lead to unrealistic emissions in certain locations (e.g., the inclusion of shrubs EF into grasses EF) and discrepancies between different modelling approaches (e.g., UKESM1 versus CESM). Assessment of the impact of using a wider range of PFTs, based on more highly resolved emission factor datasets (e.g., Karl et al., 2009), would be informative.

The expansion of iBVOC to speciate terpenes into separate α-pinene and β-pinene tracers and the addition of new molecules, such as sesquiterpenes, would be beneficial for simulating atmospheric composition. α-pinene and β-pinene display different chemical reactivity while sesquiterpenes can suppresses local O_3 and affect SOA formation by producing highly involatile species which can nucleate new particles without sulphuric acid (e.g., Bianchi et al., 2019; Weber et al., 2020).

5 Conclusions

The influence of BVOC emissions on atmospheric composition and climate and the predicted changes in these emissions from climatic and land use drivers means accurate modelling is critical for understanding past, present, and future climate.

In this study we have described the development and evaluation of alternative sets of emissions factors (EF_{mass}) for isoprene and monoterpenes from the established MEGAN v2.1 scheme. This development rectifies the issue in the current UKESM1 setup of the over contribution to total isoprene emissions from C4 PFTs, caused by the differences in the scope of vegetation types included in the C3 and C4 PFTs in UKESM1 and the previous source of emissions factors, ORCHIDEE. The correction reduces the C4 grass' contribution to total isoprene emissions, bringing them into line with other literature. Meanwhile EF_{mass} values for isoprene and terpene increase for the three broadleaf tree PFTs in UKESM1. This leads to the fraction of both isoprene and terpene produced by the tropical broadleaf evergreen tree increasing from ~50% to ~80%.

During the calculation we identified variation in SLW datasets and the decision about which monoterpene emission factors to use as sources of uncertainty in the final EF_{mass} values. The high bias in simulated isoprene columns values increases slightly with the updated IEF_{mass} values compared to UKESM1 approach although this change is much smaller than that caused by switching between chemical mechanisms.

When using the current UKESM1 EF_{mass} values, isoprene emissions decrease in future LULC scenario featuring widescale tree planting relative to 2010 levels due to the erroneously high IEF_{mass} of C4 grass. When the new EF_{mass} values are used, isoprene emission increase and UKESM's response agrees closely with the response simulated by CESM. Thus, the increase in EF_{mass} for tropical trees and the reduction for C4 PFTs is likely to have consequences for the evolution of isoprene emissions under different future scenarios given the competition between C4 PFTs and tropical broadleaf evergreen trees (e.g., cropland expansion vs. re/afforestation efforts).

Author Contributions

JW calculated the new EF, with advice from KS, and performed the UKESM1 model simulations. JAK performed the CESM model simulations. JW analysed all the model simulations and JW, JAK and MVM discussed the model output.

Acknowledgements

This work used Monsoon2, a collaborative high-performance computing facility funded by the Met Office and the Natural Environment Research Council. This work used JASMIN, the UK collaborative data analysis facility. This work was supported by the UKRI Future Leaders Fellowship Programme awarded to MVM (MR/T019867/1). High-performance computing support from Cheyenne (doi:10.5065/D6RX99HX) was provided by NCAR's Computational and Information Systems Laboratory, sponsored by the National Science Foundation.

Data and Code Availability

The UKESM1 model data generated for this work and the code used to analyse it are available at the following repository 10.5281/zenodo.7741131.

Simulations used in this work were performed using version 12.0 of the Met Office Unified Model (UM) and vn5.6 of the Joint United Kingdom Land Environment Simulator (JULES). Details of how to access and run the model can be found at https://cms.ncas.ac.uk/unified-model/configurations/ukesm/relnotes-1.0/amip/.

Due to intellectual property right restrictions, we cannot provide either the source code or documentation papers for the UM. The Met Office United Model is available for use under licence. A number of research organizations and national meteorological services use the UM in collaboration with the UK Met Office to undertake basic atmospheric process research, produce forecasts, develop the UM code, and build and evaluate Earth system models. No UM/UKESM1 code has been changed for this study, only the emission factor parameters, and Pacifico et al. (2011) provides a full explanation of the relevant equations used to model emissions in UKESM1. For further information on how to apply for a licence, see https://www.metoffice.gov.uk/research/approach/modelling-systems/unified-model (last access: 3rd May 2022).

The UM and/or JULES code branch(es) used in the publication have not all been submitted for review and inclusion in the UM/JULES trunk or released for general use. However, the UM and JULES code branches were made available to reviewers of this manuscript.

References

Ali, A. A., Xu, C., Rogers, A., Fisher, R. A., Wullschleger, S. D., Massoud, E. C., Vrugt, J. A., Muss, J. D., McDowell, N. G.,
730   Fisher, J. B., Reich, P. B., and Wilson, C. J.: A global scale mechanistic model of photosynthetic capacity (LUNA V1.0),
Geosci. Model Dev., 9, 587–606, https://doi.org/10.5194/gmd-9-587-2016, 2016.

Archibald, A. T., O'Connor, F. M., Abraham, N. L., Archer-Nicholls, S., Chipperfield, M. P., Dalvi, M., Folberth, G. A.,
Dennison, F., Dhomse, S. S., Griffiths, P. T., Hardacre, C., Hewitt, A. J., Hill, R. S., Johnson, C. E., Keeble, J., Köhler, M. O.,
735   Morgenstern, O., Mulcahy, J. P., Ordóñez, C., Pope, R. J., Rumbold, S. T., Russo, M. R., Savage, N. H., Sellar, A., Stringer,
M., Turnock, S. T., Wild, O., and Zeng, G.: Description and evaluation of the UKCA stratosphere–troposphere chemistry
scheme (StratTrop vn 1.0) implemented in UKESM1, Geosci. Model Dev., 13, 1223–1266, https://doi.org/10.5194/gmd-13-
1223-2020, 2020.

740   Best, M. J., Pryor, M., Clark, D. B., Rooney, G. G., Essery, R. L. H., Ménard, C. B., Edwards, J. M., Hendry, M. A., Porson,
A., Gedney, N., Mercado, L. M., Sitch, S., Blyth, E., Boucher, O., Cox, P. M., Grimmond, C. S. B., and Harding, R. J.: The
Joint UK Land Environment Simulator (JULES), model description – Part 1: Energy and water fluxes, Geosci. Model Dev.,
4, 677–699, https://doi.org/10.5194/gmd-4-677-2011, 2011.

745   Bianchi, F., Kurtén, T., Riva, M., Mohr, C., Rissanen, M. P., Roldin, P., Berndt, T., Crounse, J. D., Wennberg, P. O., Mentel,
T. F., and Wildt, J.: Highly oxygenated organic molecules (HOM) from gas-phase autoxidation involving peroxy radicals: A
key contributor to atmospheric aerosol, Chem. Rev., 119, 3472–3509, https://doi.org/10.1021/acs.chemrev.8b00395, 2019.

Cao, Y., Yue, X., Liao, H., Yang, Y., Zhu, J., Chen, L., Tian, C., Lei, Y., Zhou, H. and Ma, Y.: Ensemble projection of global
750   isoprene emissions by the end of 21st century using CMIP6 models. Atmospheric Environment, 118766,
https://doi.org/10.1016/j.atmosenv.2021.118766, 2021.
Clark, D. B., Mercado, L. M., Sitch, S., Jones, C. D., Gedney, N., Best, M. J., Pryor, M., Rooney, G. G., Essery, R. L. H.,
Blyth, E., Boucher, O., Harding, R. J., Huntingford, C., and Cox, P. M.: The Joint UK Land Environment Simulator (JULES),
model description – Part 2: Carbon fluxes and vegetation dynamics, Geosci. Model Dev., 4, 701–722,
755   https://doi.org/10.5194/gmd-4-701-2011, 2011.

Danabasoglu, G., Lamarque, J.F., Bacmeister, J., Bailey, D.A., DuVivier, A.K., Edwards, J., Emmons, L.K., Fasullo, J., Garcia,
R., Gettelman, A. and Hannay, C.: The community earth system model version 2 (CESM2). *Journal of Advances in Modeling
Earth Systems*, *12*, 2, p.e2019MS001916, https://doi.org/10.1029/2019MS001916, 2020.
760

Dee, D. P., Uppala, S. M., Simmons, A. J., Berrisford, P., Poli, P., Kobayashi, S., Andrae, U., Balmaseda, M. A., Balsamo, G., Bauer, P., Bechtold, P., Beljaars, A. C. M., van de Berg, L., Bidlot, J., Bormann, N., Delsol, C., Dragani, R., Fuentes, M., Geer, A. J., Haimberger, L., Healy, S. B., Hersbach, H., Hólm, E. V., Isaksen, L., Kållberg, P., Köhler, M., Matricardi, M., McNally, A. P., Monge-Sanz, B. M., Morcrette, J.-J., Park, B.-K., Peubey, C., de Rosnay, P., Tavolato, C., Thépaut, J.-N., and Vitart, F.: The ERA-Interim reanalysis: configuration and performance of the data assimilation system, Q. J. Roy. Meteor. Soc., 137, 553–597,https://doi.org/10.1002/qj.828, 2011.

Emmons, L.K., Orlando, J.J., Tyndall, G., Schwantes, R.H., Kinnison, D.E., Marsh, D.R. and Mills, M.J., Tilmes., S., and Lamarque, J.-F.: The MOZART Chemistry Mechanism in the Community Earth System Model version 2 (CESM2). *J. Adv. Model. Earth Syst*, *12,* 10.1029, https://doi.org/10.1029/2019MS001882, 2020.

Guenther, A., Hewitt, C. N., Erickson, D., Fall, R., Geron, C., Graedel, T., Harley, P., Klinger, L., Lerdau, M., Mckay, W. A., Pierce, T., Scholes, B., Steinbrecher, R., Tallamraju, R., Tay- lor, J., and Zimmerman, P.: A global model of natural volatile organic compound emissions, J. Geophys. Res., 100, D5, 8873– 8892, https://doi.org/10.1029/94JD02950, 1995.

Guenther, A., Baugh, W., Davis, K., Hampton, G., Harley, P., Klinger, L., Vierling, L., Zimmerman, P., Allwine, E., Dilts, S. and Lamb, B.: Isoprene fluxes measured by enclosure, relaxed eddy accumulation, surface layer gradient, mixed layer gradient, and mixed layer mass balance techniques. Journal of Geophysical Research: Atmospheres, 101, D13, 18555-18567, https://doi.org/10.1029/96JD00697, 1996.

Guenther, A., Archer, S., Harley, P., Helmig, D., Klinger, L., Vier- ling, L., Wildermuth, M., Zimmerman, P., and Zitzer, S.: Bio- genic hydrocarbon emissions and landcover/climate change in a subtropical savanna, Phys. Chem. Earth, 24, 6, 659–667, https://doi.org/10.1016/S1464-1909(99)00062-3, 1999.

Guenther, A., Karl, T., Harley, P., Wiedinmyer, C., Palmer, P. I., and Geron, C.: Estimates of global terrestrial isoprene emissions using MEGAN (Model of Emissions of Gases and Aerosols from Nature), Atmos. Chem. Phys., 6, 3181–3210, https://doi:10.5194/acp-6-3181-2006, 2006.

Guenther, A. B., Jiang, X., Heald, C. L., Sakulyanontvittaya, T., Duhl, T., Emmons, L. K., and Wang, X.: The Model of Emissions of Gases and Aerosols from Nature version 2.1 (MEGAN2.1): an extended and updated framework for modeling biogenic emissions, Geosci. Model Dev., 5, 1471–1492, https://doi.org/10.5194/gmd-5-1471-2012, 2012.

Harley, P., Otter, L., Guenther, A. and Greenberg, J.:. Micrometeorological and leaf-level measurements of isoprene emissions from a southern African savanna. *Journal of Geophysical Research: Atmospheres*, *108*, D13, https://doi.org/10.1029/2002JD002592, 2003.

Hoesly, R. M., Smith, S. J., Feng, L., Klimont, Z., Janssens-Maenhout, G., Pitkanen, T., Seibert, J. J., Vu, L., Andres, R. J., Bolt, R. M., Bond, T. C., Dawidowski, L., Kholod, N., Kurokawa, J.-I., Li, M., Liu, L., Lu, Z., Moura, M. C. P., O'Rourke, P. R., and Zhang, Q.: Historical (1750–2014) anthropogenic emissions of reactive gases and aerosols from the Community Emissions Data System (CEDS), Geosci. Model Dev., 11, 369–408, https://doi.org/10.5194/gmd-11-369-2018, 2018.

Jenkin, M. E., Khan, M. A. H., Shallcross, D. E., Bergström, R., Simpson, D., Murphy, K. L. C., and Rickard, A. R.: The CRI v2. 2 reduced degradation scheme for isoprene, Atmos. Environ., 212, 172–182, https://doi.org/10.1016/j.atmosenv.2019.05.055, 2019.

Karl, M., Guenther, A., Köble, R., Leip, A., and Seufert, G.: A new European plant-specific emission inventory of biogenic volatile organic compounds for use in atmospheric transport models, Biogeosciences, 6, 1059–1087, https://doi.org/10.5194/bg-6-1059-2009, 2009.

Klinger, L.F., Greenburg, J., Guenther, A., Tyndall, G., Zimmerman, P., M'bangui, M., Moutsamboté, J.M. and Kenfack, D.: Patterns in volatile organic compound emissions along a savanna-rainforest gradient in central Africa. Journal of Geophysical Research: Atmospheres, 103, D1, 1443-1454, https://doi.org/10.1029/97JD02928, 1998.

Lathière, J., Hauglustaine, D. A., Friend, A. D., De Noblet-Ducoudré, N., Viovy, N., and Folberth, G. A.: Impact of climate variability and land use changes on global biogenic volatile organic compound emissions, Atmos. Chem. Phys., 6, 2129–2146, https://doi.org/10.5194/acp-6-2129-2006, 2006.

Lawrence, D.M., Oleson, K.W., Flanner, M.G., Thornton, P.E., Swenson, S.C., Lawrence, P.J., Zeng, X., Yang, Z.L., Levis, S., Sakaguchi, K. and Bonan, G.B.: Parameterization improvements and functional and structural advances in version 4 of the Community Land Model. Journal of Advances in Modeling Earth Systems, 3, 1, https://doi.org/10.1029/2011MS00045, 2011.

Lawrence, D.M., Fisher, R.A., Koven, C.D., Oleson, K.W., Swenson, S.C., Bonan, G., Collier, N., Ghimire, B., van Kampenhout, L., Kennedy, D. and Kluzek, E., 2019. The Community Land Model version 5: Description of new features, benchmarking, and impact of forcing uncertainty. Journal of Advances in Modeling Earth Systems, 11, 12, 4245-4287, https://doi.org/10.1029/2018MS001583, 2019.

Liu, X., Ma, P.-L., Wang, H., Tilmes, S., Singh, B., Easter, R. C., Ghan, S. J., and Rasch, P. J.: Description and evaluation of a new four-mode version of the Modal Aerosol Module (MAM4) within version 5.3 of the Community Atmosphere Model, Geosci. Model Dev., 9, 505–522, https://doi.org/10.5194/gmd-9-505-2016, 2016.

830

Loreto, F. and Fineschi, S.: Reconciling functions and evolution of isoprene emission in higher plants. New Phytologist, 206, 2, 578-582, https://doi.org/10.1111/nph.13242, 2015.

Meinshausen, M., Vogel, E., Nauels, A., Lorbacher, K., Meinshausen, N., Etheridge, D. M., Fraser, P. J., Montzka, S. A.,
835 Rayner, P. J., Trudinger, C. M., Krummel, P. B., Beyerle, U., Canadell, J. G., Daniel, J. S., Enting, I. G., Law, R. M., Lunder, C. R., O'Doherty, S., Prinn, R. G., Reimann, S., Rubino, M., Velders, G. J. M., Vollmer, M. K., Wang, R. H. J., and Weiss, R.: Historical greenhouse gas concentrations for climate modelling (CMIP6), Geosci. Model Dev., 10, 2057–2116, https://doi.org/10.5194/gmd-10-2057-2017, 2017.

840 Messina, P., Lathière, J., Sindelarova, K., Vuichard, N., Granier, C., Ghattas, J., Cozic, A., and Hauglustaine, D. A.: Global biogenic volatile organic compound emissions in the ORCHIDEE and MEGAN models and sensitivity to key parameters, Atmos. Chem. Phys., 16, 14169–14202, https://doi.org/10.5194/acp-16-14169-2016, 2016.

Mulcahy, J. P., Johnson, C., Jones, C. G., Povey, A. C., Scott, C. E., Sellar, A., Turnock, S. T., Woodhouse, M. T., Abraham,
845 N. L., Andrews, M. B., Bellouin, N., Browse, J., Carslaw, K. S., Dalvi, M., Folberth, G. A., Glover, M., Grosvenor, D. P., Hardacre, C., Hill, R., Johnson, B., Jones, A., Kipling, Z., Mann, G., Mollard, J., O'Connor, F. M., Palmiéri, J., Reddington, C., Rumbold, S. T., Richardson, M., Schutgens, N. A. J., Stier, P., Stringer, M., Tang, Y., Walton, J., Woodward, S., and Yool, A.: Description and evaluation of aerosol in UKESM1 and HadGEM3-GC3.1 CMIP6 historical simulations, Geosci. Model Dev., 13, 6383–6423, https://doi.org/10.5194/gmd-13-6383-2020, 2020.

850

Olivier, J. G. J., Peters, J., Granier, C., Petron, G., Muller, J.-F., and Wallens, S.: Present and future surface emissions of atmospheric compounds, POET Report #3, EU project EVK2-1999-00011, available at: http://www.aero.jussieu.fr/projet/ACCENT/Documents/del2_final.doc (last access: 18 June 2022), 2003.

855 O'Neill, B. C., Tebaldi, C., van Vuuren, D. P., Eyring, V., Friedling- stein, P., Hurtt, G., Knutti, R., Kriegler, E., Lamarque, J.-F., Lowe, J., Meehl, G. A., Moss, R., Riahi, K., and Sander- son, B. M.: The Scenario Model Intercomparison Project (Sce-narioMIP) for CMIP6, Geosci. Model Dev., 9, 3461–3482, doi:10.5194/gmd-9-3461-2016, 2016.

Otter, L.B., Guenther, A. and Greenberg, J.: Seasonal and spatial variations in biogenic hydrocarbon emissions from southern African savannas and woodlands. Atmospheric Environment, 36, 26, 4265-4275, https://doi.org/10.1016/S1352-2310(02)00333-3, 2002.

Pacifico, F., Harrison, S. P., Jones, C. D., Arneth, A., Sitch, S., Weedon, G. P., Barkley, M. P., Palmer, P. I., Serça, D., Potosnak, M., Fu, T.-M., Goldstein, A., Bai, J., and Schurgers, G.: Evaluation of a photosynthesis-based biogenic isoprene emission scheme in JULES and simulation of isoprene emissions under present-day climate conditions, Atmos. Chem. Phys., 11, 4371–4389, https://doi.org/10.5194/acp-11-4371-2011, 2011.

Peeters, J., Nguyen, T. L., and Vereecken, L.: HO_x radical regeneration in the oxidation of isoprene, Phys. Chem. Chem. Phys., 11, 5935–5939, https://doi.org/10.1039/B908511D, 2009.

Pfister, G.G., Emmons, L.K., Hess, P.G., Lamarque, J.F., Orlando, J.J., Walters, S., Guenther, A., Palmer, P.I. and Lawrence, P.J.: Contribution of isoprene to chemical budgets: A model tracer study with the NCAR CTM MOZART-4. Journal of Geophysical Research: Atmospheres, 113, D5, https://doi.org/10.1029/2007JD008948, 2005.

Schurgers, G., Arneth, A., Holzinger, R., and Goldstein, A. H.: Process-based modelling of biogenic monoterpene emissions combining production and release from storage, Atmos. Chem. Phys., 9, 3409–3423, https://doi.org/10.5194/acp-9-3409-2009, 2009.

Schwantes, R. H., Emmons, L. K., Orlando, J. J., Barth, M. C., Tyndall, G. S., Hall, S. R., Ullmann, K., St. Clair, J. M., Blake, D. R., Wisthaler, A., and Bui, T. P. V.: Comprehensive isoprene and terpene gas-phase chemistry improves simulated surface ozone in the southeastern US, Atmos. Chem. Phys., 20, 3739–3776, https://doi.org/10.5194/acp-20-3739-2020, 2020.

Sellar, A. A., Walton, J., Jones, C. G., Wood, R., Abraham, N. L., Andrejczuk, M., Andrews, M. B., Andrews, T., Archibald, A. T., de Mora, L., and Dyson, H.: Implementation of UK Earth system models for CMIP6, J. Adv. Model. Earth Sy., 12, e2019MS00194, https://doi.org/10.1029/2019MS001946, 2020.

Sindelarova, K., Granier, C., Bouarar, I., Guenther, A., Tilmes, S., Stavrakou, T., Müller, J.-F., Kuhn, U., Stefani, P., and Knorr, W.: Global data set of biogenic VOC emissions calculated by the MEGAN model over the last 30 years, Atmos. Chem. Phys., 14, 9317–9341, https://doi.org/10.5194/acp-14-9317-2014, 2014.

Sindelarova, K., Markova, J., Simpson, D., Huszar, P., Karlicky, J., Darras, S., and Granier, C.: High-resolution biogenic global emission inventory for the time period 2000–2019 for air quality modelling, Earth Syst. Sci. Data, 14, 251–270, https://doi.org/10.5194/essd-14-251-2022, 2022.

895

Thornhill, G., Collins, W., Olivié, D., Skeie, R. B., Archibald, A., Bauer, S., Checa-Garcia, R., Fiedler, S., Folberth, G., Gjermundsen, A., Horowitz, L., Lamarque, J.-F., Michou, M., Mulcahy, J., Nabat, P., Naik, V., O'Connor, F. M., Paulot, F., Schulz, M., Scott, C. E., Séférian, R., Smith, C., Takemura, T., Tilmes, S., Tsigaridis, K., and Weber, J.: Climate-driven chemistry and aerosol feedbacks in CMIP6 Earth system models, Atmos. Chem. Phys., 21, 1105–
900 1126, https://doi.org/10.5194/acp-21-1105-2021, 2021.

Walters, D., Baran, A. J., Boutle, I., Brooks, M., Earnshaw, P., Edwards, J., Furtado, K., Hill, P., Lock, A., Manners, J., Morcrette, C., Mulcahy, J., Sanchez, C., Smith, C., Stratton, R., Tennant, W., Tomassini, L., Van Weverberg, K., Vosper, S., Willett, M., Browse, J., Bushell, A., Carslaw, K., Dalvi, M., Essery, R., Gedney, N., Hardiman, S., Johnson, B., Johnson, C.,
905 Jones, A., Jones, C., Mann, G., Milton, S., Rumbold, H., Sellar, A., Ujiie, M., Whitall, M., Williams, K., and Zerroukat, M.: The Met Office Unified Model Global Atmosphere 7.0/7.1 and JULES Global Land 7.0 configurations, Geosci. Model Dev., 12, 1909–1963, https://doi.org/10.5194/gmd-12-1909-2019, 2019.

Weber, J., Archer-Nicholls, S., Griffiths, P., Berndt, T., Jenkin, M., Gordon, H., Knote, C., and Archibald, A. T.: CRI-HOM:
910 A novel chemical mechanism for simulating highly oxygenated organic molecules (HOMs) in global chemistry–aerosol–climate models, Atmos. Chem. Phys., 20, 10889–10910, https://doi.org/10.5194/acp-20-10889-2020, 2020.

Weber, J., Archer-Nicholls, S., Abraham, N. L., Shin, Y. M., Bannan, T. J., Percival, C. J., Bacak, A., Artaxo, P., Jenkin, M., Khan, M. A. H., Shallcross, D. E., Schwantes, R. H., Williams, J., and Archibald, A. T.: Improvements to the representation
915 of BVOC chemistry–climate interactions in UKCA (v11.5) with the CRI-Strat 2 mechanism: incorporation and evaluation, Geosci. Model Dev., 14, 5239–5268, https://doi.org/10.5194/gmd-14-5239-2021, 2021.

Weber, J., Archer-Nicholls, S., Abraham, N.L., Shin, Y. M., Grosvenor, D.P., Scott, C. E and Archibald, A. T.: Chemistry-driven changes strongly influence climate forcing from vegetation emissions. Nature Communications **13**, 7202,
920 https://doi.org/10.1038/s41467-022-34944-9, 2022.

Wells, K. C., Millet, D. B., Payne, V. H., Deventer, M. J., Bates, K. H., de Gouw, J. A., Graus, M., Warneke, C., Wisthaler, A., and Fuentes, J. D.: Satellite isoprene retrievals constrain emissions and atmospheric oxidation, Nature, 585, 225–233, https://doi.org/10.1038/s41586-020-2664-3, 2020.

Wennberg, P. O., Bates, K. H., Crounse, J. D., Dodson, L. G., McVay, R. C., Mertens, L. A., Nguyen, T. B., Praske, E.,
Schwantes, R. H., Smarte, M. D., and St Clair, J. M.: Gas-phase reactions of isoprene and its major oxidation products, Chem.
Rev., 118, 3337-3390, https://doi.org/10.1021/acs.chemrev.7b00439, 2018.

Woodward, S.: Modelling the atmospheric life cycle and radiative impact of mineral dust in the Hadley Cen- tre climate model,
J. Geophys. Res., 106, 18155–18166, https://doi.org/10.1029/2000JD900795, 2001.

Yáñez-Serrano, A.M., Bourtsoukidis, E., Alves, E.G., Bauwens, M., Stavrakou, T., Llusià, J., Filella, I., Guenther, A.,
Williams, J., Artaxo, P. and Sindelarova, K.: Amazonian biogenic volatile organic compounds under global change. *Global
change biology*, *26*, 9, 4722-4751, https://doi.org/10.1111/gcb.15185, 2020.

Zhang, M., Zhao, C., Yang, Y., Du, Q., Shen, Y., Lin, S., Gu, D., Su, W., and Liu, C.: Modeling sensitivities of BVOCs to
different versions of MEGAN emission schemes in WRF-Chem (v3.6) and its impacts over eastern China, Geosci. Model
Dev., 14, 6155–6175, https://doi.org/10.5194/gmd-14-6155-2021, 2021.
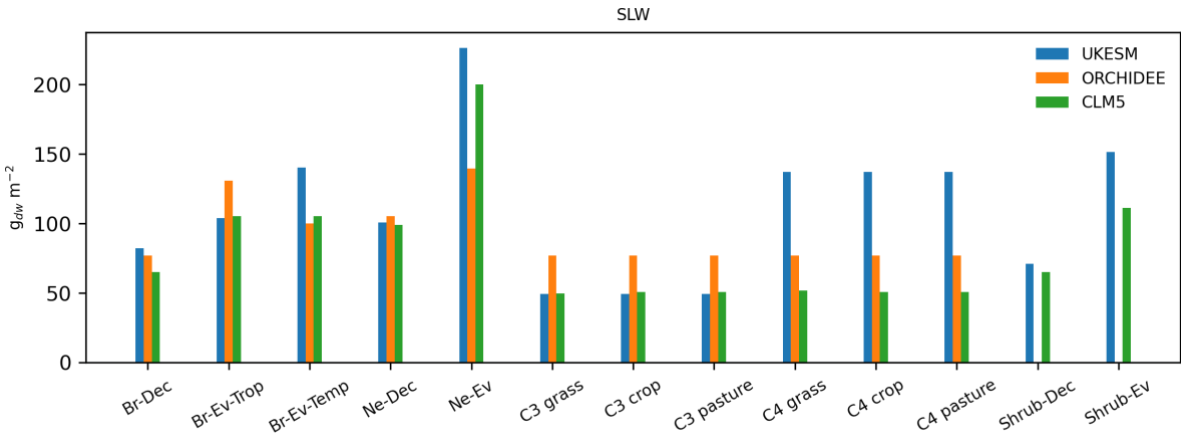
**Figure 1. SLW values for UKESM1 PFTs from the UKESM1, ORCHIDEE and CLM5 datasets. ORCHIDEE does
not consider shrubs as separate PFTs so there are no corresponding SLW values.**
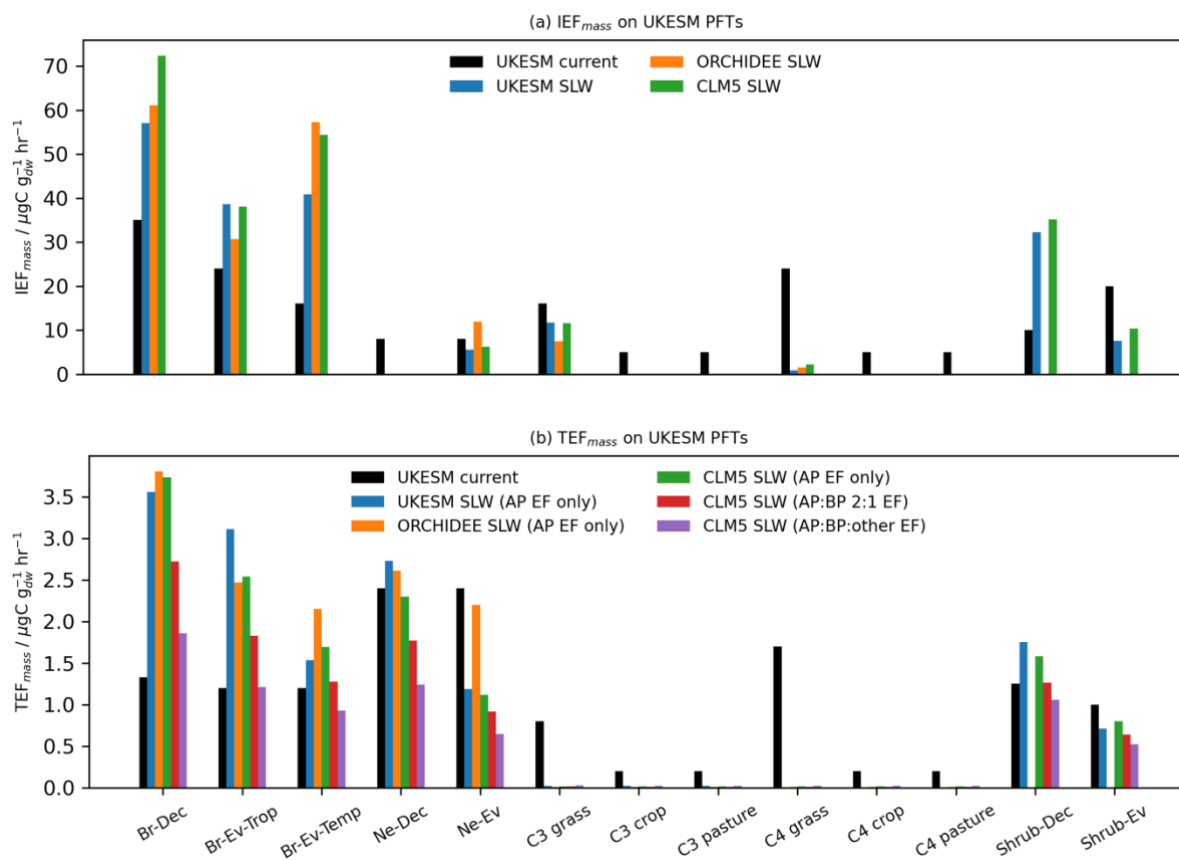
945 **Figure 2. Default and new (a) IEF$_{mass}$ and (b) TEF$_{mass}$ for UKESM1 PFTs.**
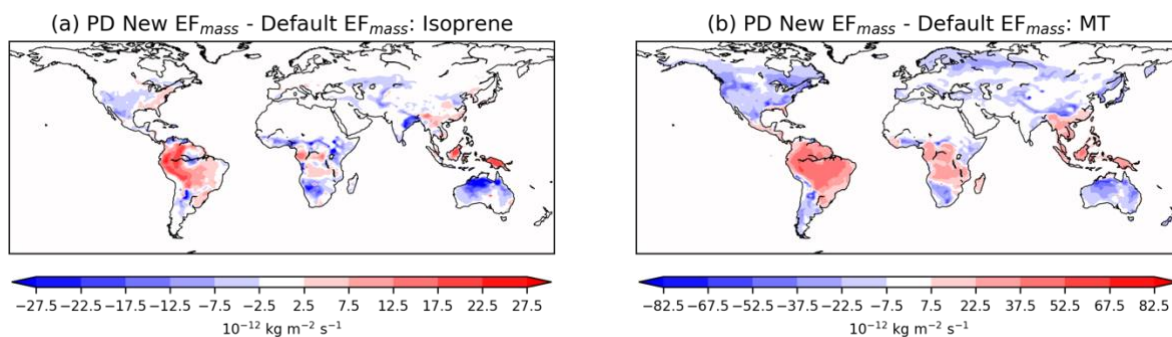
950 **Figure 3. 3-year annual average change in (a) isoprene and (b) monoterpene (MT) emissions following the change in EF$_{mass}$ values.**
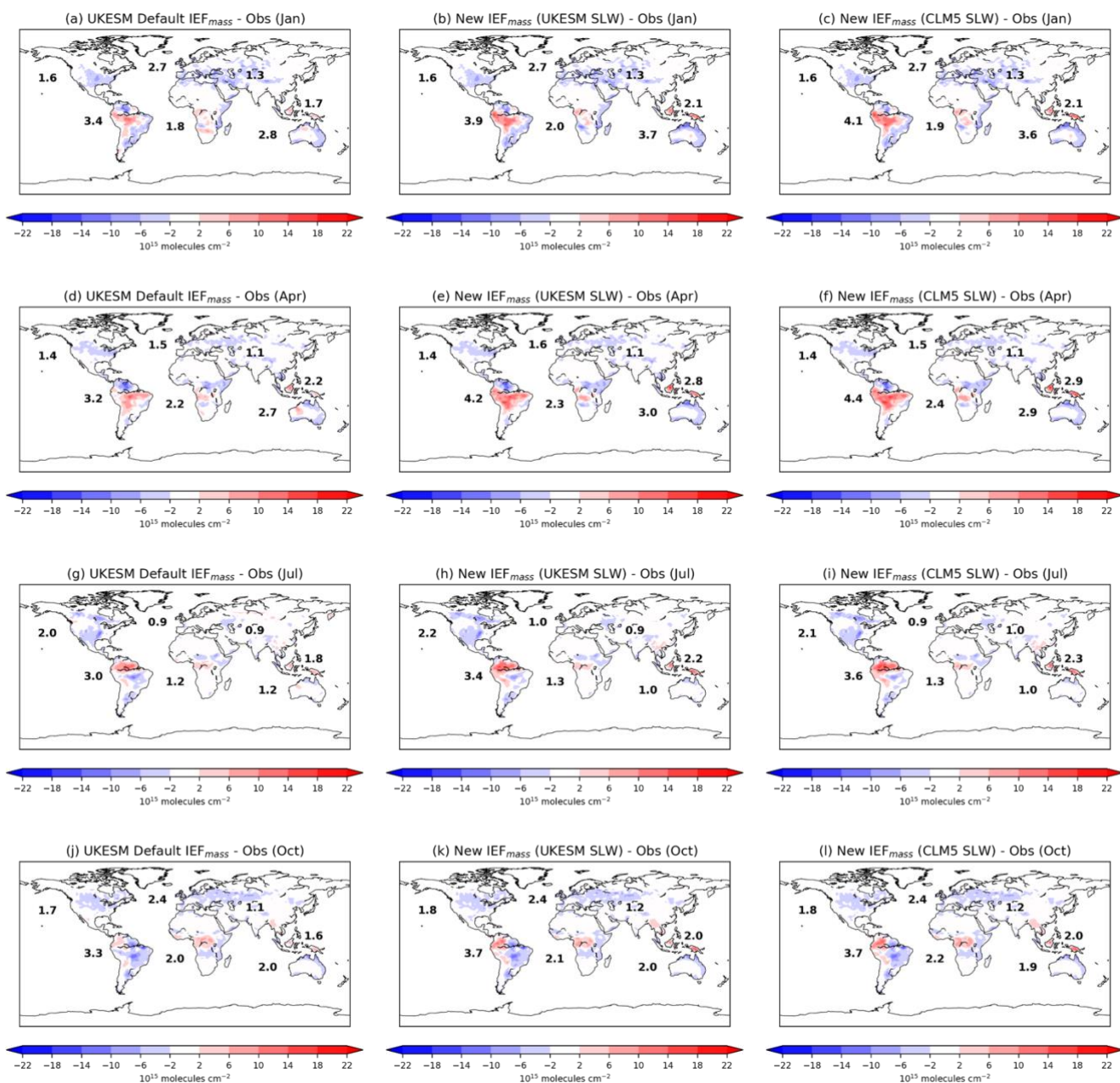
Figure 4. Modelled isoprene column compared to observational data (Wells et al., 2020) for (a-c) January 2013, (d-f) April 2013, (g-i) July 2013 and (j-l) October 2013. Model data from UKESM1 IEF$_{mass}$ New IEF$_{mass}$ (UKESM1 SLW) and New IEF$_{mass}$ (CLM5 SLW) from Control_1yr_PD, IEF_SLW_UKESM_PD and IEF_SLW_CLM5_PD simulations respectively. Numbers show mean absolute bias (MAB = |model – obs|) weighted by area for each continent (African value excludes the Sahara).
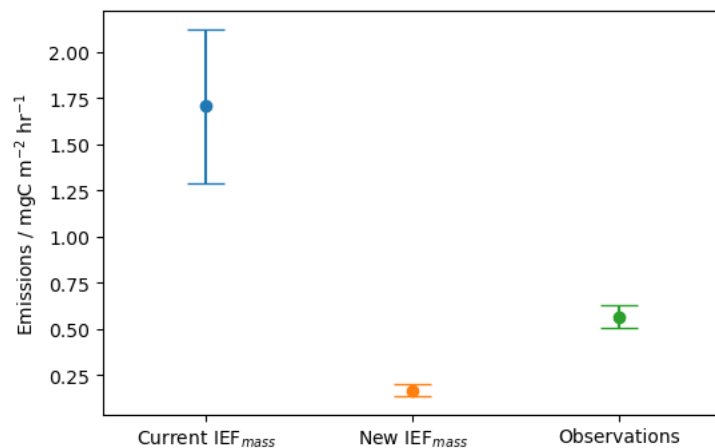
Figure 5. Simulated isoprene emissions from the IEF_{mass} currently used in UKESM1 and the new IEF_{mass} described in this study and observations. For the simulated emissions we only consider grid cells with > 80% C4 grass located in the same regions as the observations.
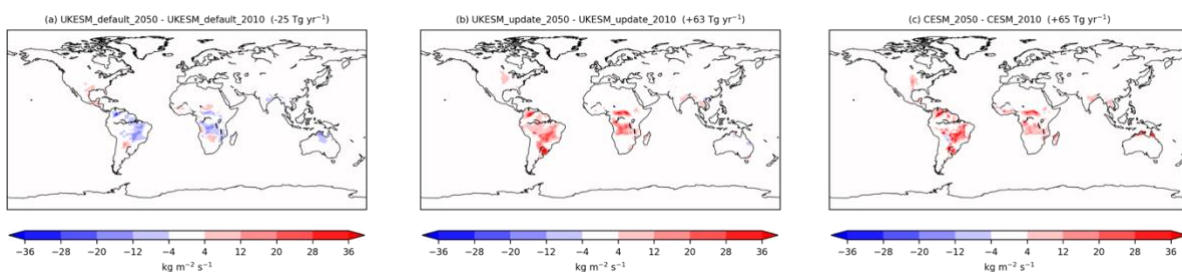
Figure 6. Annual mean change (2050 minus 2010) in isoprene emissions in (a) original UKESM1, (b) UKESM1 with new IEF_{mass} and (c) CESM2 following widespread tree planting under the Maxforest scenario. Values in parentheses show global mean difference in emissions.

Table 1. IEF in 5-PFT setup

PFT	IEF$_{mass}$ / µgC g$_{dw}^{-1}$ hr^{-1}
Broadleaf trees	35
Needleleaf trees	12
C3 grass	16
C4 grass	8
Shrubs	20

975

Table 2. IEF$_{mass}$ (in µgC g$_{dw}^{-1}$ hr^{-1}) in 13-PFT setup of UKESM1

PFT	Abbreviation	iBVOC Std	ORCHIDEEv1[a]	ORCHIDEE v2[b]
Broadleaf deciduous trees	Br-Dec	35	24/45/8[c]	24/45/18[c]
Broadleaf evergreen tropical trees	Br-Ev-Trop	24	24	24
Broadleaf evergreen temperate trees	Br-Ev-Temp	16	16	16
Needleleaf deciduous trees	Ne-Dec	8	8	0.5
Needleleaf evergreen trees	Ne-Ev	8	8/8[d]	8/8[d]
C3 grass	C3 grass	16	16	12
C3 crop	C3 crop	5	5	5
C3 pasture	C3 pasture	5	5	5
C4 grass	C4 grass	24	24	18
C4 crop	C4 crop	5	5	5
C4 pasture	C4 pasture	5	5	5
Shrub deciduous	Shrub-Dec	10	Not in scheme	Not in scheme
Shrub evergreen	Shrub-Ev	20	Not in scheme	Not in scheme

[a] **Lathière et al (2006)**

[b]Messina et al (2016)

980   [c]tropical / temperate / boreal, area-weighted mean

[d]temperate / boreal

Table 3. MEGAN PFTs and corresponding UKESM1 PFTs.

MEGAN PFT(s)	UKESM1 PFT
Direct Equivalent	
Tropical broadleaf evergreen	Tropical broadleaf evergreen
Temperate broadleaf evergreen	Temperate broadleaf evergreen
Needleleaf deciduous	Needleleaf deciduous
C4 grass	C4 grass
Broadleaf evergreen shrub temperate	Shrub evergreen
Lumped Species	
Needleleaf evergreen temperate Needleleaf evergreen boreal	Needleleaf evergreen
Broadleaf deciduous tropical Broadleaf deciduous temperate Broadleaf deciduous boreal	Broadleaf deciduous
C3 grass C3 arctic grass	C3 Grass
Broadleaf deciduous temperate shrub Broadleaf deciduous boreal shrub	Shrub deciduous
Crops	
C1	C3 crop, C3 pasture, C4 crop, C4 pasture

985

Table 4. Evaluation Simulations with UKESM1. Reported are the average for 1-year simulations and the average and range of annual means (in parentheses) for multi-year simulations. The UKESM1.0 simulations used UM version 12.0.

Simulation	Run Specifications	IEF$_{mass}$	TEF$_{mass}$	Global Isoprene Emissions / Tg yr^{-1}	Global Terpene Emissions / Tg yr^{-1}
Nudged PD Simulations					
Control_1yr_PD	Nov 2012 – Oct 2013 UKESM1 LULC	UKESM1 Default	UKESM1 Default	527	138
No_C4_emiss_PD	Nov 2012 – Oct 2013 UKESM1 LULC	UKESM1 Default w/ all C4 IEF=0	UKESM1 Default w/ all C4 TEF=0	312	113
IEF_SLW_UKESM_PD	Nov 2012 – Oct 2013 UKESM1 LULC	Updated SLW: UKESM1	UKESM1 Default	457	138
IEF_SLW_CLM5_PD	Nov 2012 – Oct 2013 UKESM1 LULC	Updated SLW: CLM5	UKESM1 Default	491	138
IEF_SLW_UKESM_PD_CESM_LULC	Nov 2012 – Oct 2013 CESM2 LULC	Updated SLW: UKESM1	UKESM1 Default	380	97
IEF_SLW_CLM5_PD_CESM_LULC	Nov 2012 – Oct 2013 CESM2 LULC	Updated SLW: CLM5	UKESM1 Default	420	97
TEF_AP_PD	Nov 2012 – Oct 2013 UKESM1 LULC	Updated SLW: CLM5	Updated SLW: CLM5 EF: AP only	488	177
TEF_AP_BP_PD	Nov 2012 – Oct 2013 UKESM1 LULC	Updated SLW: CLM5	Updated SLW: CLM5 EF: AP/BP/ 2:1	489	130
TEF_all_PD	Nov 2012 – Oct 2013 UKESM1 LULC	Updated SLW: CLM5	Updated SLW: CLM5 EF: AP/BP/other	491	88
Control_3yr_PD	2005-2007	UKESM1 Default	UKESM1 Default	545 (539-551)	140 (138-141)
Proposed_EF_3yr_PD	2005-2007	Updated SLW: CLM5	Updated SLW: CLM5 EF: AP/BP/other	498 (493 – 505)	130 (127-131)
Free Running Simulations					

Base PI	3-year PI UKESM1 LULC, SSTs and emissions	UKESM1 Default	UKESM1 Default	744 (742-747)	140 (139-141)
Updated EF PI	3-year PI UKESM1 LULC, SSTs and emissions	Updated SLW: CLM5	Updated SLW: CLM5 EF: AP/BP/other	645 (637-649)	125 (125-125)
Base 2050 SSP3-7.0	3-year 2050 SSP3-7.0 UKESM1 LULC, SSTs and emissions	UKESM1 Default	UKESM1 Default	603 (591-612)	178 (177-179)
Updated EF 2050 SSP3-7.0	3-year 2050 SSP3-7.0 UKESM1 LULC, SSTs and emissions	Updated SLW: CLM5	Updated SLW: CLM5 EF: AP/BP/other	556 (553 – 560)	163 (162-164)

990

Table 5. Evaluation atmosphere-only simulations with UKESM1 and CESM performed to investigate response to LULC change with different EF. The UKESM1.0 simulations use UM version 12.0. All simulations use SSTs from SSP3-7.0 at 2050 and WMGHGs and anthropogenic and biomass burning emissions from 2010.

Simulation	Model	IEF	TEF	Land Use
UKESM_default_2010	UKESM	UKESM1 default	UKESM1 default	2010
UKESM_default_2050	UKESM	UKESM1 default	UKESM1 default	2050 Maxforest
UKESM_update_2010	UKESM	Updated SLW: CLM5	Updated SLW: CLM5 EF: AP/BP/ 2:1	2010
UKESM_ update _2050	UKESM	Updated SLW: CLM5	Updated SLW: CLM5 EF: AP/BP/ 2:1	2050 Maxforest
CESM_2010	CESM	CESM default (MEGAN v2.1)	CESM default (MEGAN v2.1)	2010
CESM_2050	CESM	CESM default (MEGAN v2.1)	CESM default (MEGAN v2.1)	2050 Maxforest

995 **Table 6. Recommended EF_{mass} ($\mu gC\ g_{dw}^{-1}\ hr^{-1}$) for use in iBVOC**

UKESM1 PFT	IEF_{mass}	TEF_{mass}
Broadleaf deciduous trees	72.3	2.7

Broadleaf evergreen tropical trees	38.1	1.8
Broadleaf evergreen temperate trees	54.4	1.3
Needleleaf deciduous trees	0.01	1.8
Needleleaf evergreen trees	6.3	0.9
C3 grass	11.6	0.02
C3 crop	0.01	0.02
C3 pasture	0.01	0.02
C4 grass	2.20	0.02
C4 crop	0.01	0.02
C4 pasture	0.01	0.02
Shrub deciduous	35.2	1.3
Shrub evergreen	10.2	0.6